408

Persistence of Laminar Flamelet Structure Under Highly Turbulent Combustion*

Kazuhiro YAMAMOTO**, Yasuki NISHIZAWA***
and Yoshiaki ONUMA***

We have investigated the premixed flame structure in highly turbulent flow with a cyclone-jet combustor. Based on the turbulent properties determined by Slot-Correlation method, the condition of $U_m < 15$ m/s belongs to the flamelet regime, and that of $U_m > 20$ m/s belongs to the distributed reaction zone regime on the combustion diagram. Also, we have quantitatively estimated the reaction zone thickness, using the probability of reaction zone existing. Results show that the dependence of reaction zone thickness on equivalence ratio is very similar to those of the experimental values by Yamaoka and Tsuji or the Zeldovich thickness. When the exit velocity is increased, the reaction zone thickness is almost constant for $Ka > 1$. Hence, the persistence of laminar flamelet structure is observed, even when the Kolmogorov scale is smaller than reaction zone thickness. It could be concluded that the reaction region remains undisturbed with thin reaction zone under highly turbulent conditions. These results are useful for modeling turbulent combustion.

Key Words: Premixed Combustion, Flame, LDV, Reaction Zone Thickness, Phase Diagram, Slot-Correlation Method

1. Introduction

For modeling turbulent combustion, numerous studies have been made[1]-[5]. In these studies, several different regimes have been proposed to classify the premixed flame structure with a phase diagram. Nowadays, the existence of distributed reaction zone regime is questionable, and a new phase diagram has been proposed to modify the flamelet region with thin-reaction-zones regime[6]-[8]. They have experimentally confirmed that the reaction region is still thin with thickened preheat zone, considering that small eddies can penetrate into the preheat zone but not into the reaction zone. For this thin-reaction-zones regime, the criteria of $l_\delta < \eta < \delta_L$ has been proposed, where l_δ is the inner layer thickness, η is the Kol-

mogorov thickness, and δ_L is the laminar flame thickness.

In the phase diagram, we usually use the laminar Zeldovich thickness by ν/S_L as flame thickness, where ν is kinetic viscosity and S_L is the laminar burning velocity. For discussion on the flame structure affected by small turbulence, we need to evaluate the reaction zone thickness. However, the flame motion is very rapid, and the reaction zone thickness is expectedly thin, less than 1 mm. A numerical simulation is a powerful tool, but until now, Large-eddy simulation (LES) is realistic system with filtered averaging[9], although some groups have simulated a three-dimensional flame with detail chemistry by DNS[10]. Still, more experimental studies are needed to evaluate numerical results.

Recently, by the drastic improvement of laser diagnostics, it has been possible to obtain two-dimensional image of flames. For example, Buschmann et al.[11] have examined the thermal structure by LIF/ Rayleigh measurements. Cheng et al. have obtained the flow and scalar fields using PIV/OH-LIF to investigate the turbulence and scalar transport[12]. Until now, there are less data available, because these laser

diagnostics are huge and very expensive system. The availability is limited. The compact system may be desirable for micro-gravity or outer space experiments.

In this study, we use an electrostatic probe to detect the reaction zone, which has high time resolution ($10^{-7} - 10^{-8}$ s[13]) enough to follow the flame fluctuation even under highly turbulent condition. Here, we determine the reaction zone thickness with probability of reaction zone existing, which is a new approach proposed in our previous study[14]. The velocity field is measured by a Laser Doppler Velocimeter (LDV). The turbulent properties are determined using Slot-Correlation method, by which the velocity fluctuation is examined directly based on randomly sampled velocity data[15]-[18].

2. Experimental

2.1 Cyclone-jet combustor

Figure 1(a) shows a cyclone-jet combustor used in this study. It is possible to investigate turbulent flames over a wide range of turbulent intensities[19],[20]. It consists of a combustion chamber with a main jet nozzle and two cyclone nozzles for pilot flames. The diameter of the main jet nozzle, d, is 12.7 mm. The cyclone combustor is of 27 mm i.d. and 23 mm height, with two cyclone nozzles of 2.4 mm i.d. For comparison, a Bunsen-type burner is also used with exit diameter of 22 mm. The fuel is propane.

Figure 1(b) shows a direct photograph of a turbulent flame obtained by this combustor. Mean exit velocity, U_m, is 10 m/s and its equivalence ratio, ϕ_m, is 0.75. Here, Z represents the axial distance from the combustor exit. Since the exposure time of this photograph is about 0.01 s, the flame structure is not clear. Then, the laser tomography technique is used to obtain the instantaneous flame image. A Nd:YAG laser (Spectra-physics GCR-170) operating at ca. 450 mJ/pulse is used to produce laser sheet of 300 μm thickness. The duration of laser pulse is 6 ns. MgO particles are used to obtain Mie-scattering image. In the experiment, we vary U_m and ϕ_m of the main jet, with a fixed condition of pilot flames for $U_p=20$ m/s and $\phi_p=0.7$ to minimize effects of pilot flames. A thermocouple is also used to specify the preheat region.

2.2 Velocity measurement

In the combustion filed, the velocity fluctuation is very large, with density change. We may use a hot wire anemometer, assuming that turbulent properties are similar to those in cold flow. However, to validate the idea that turbulent eddies do not affect the reaction zone due to the increased viscous dissipation, we need to obtain turbulent properties in combustion field. LDV is usually applied, but it is difficult to obtain correct turbulent properties based on velocity signals from particles, which are randomly sampled data[21]. Usually, in conventional data-sampling, the delay period is set to obtain the correlation between velocity data or to determine the power spectrum. Then, the interpolated velocity fluctuation does include errors, so that higher auto-correlation coefficient or unrealistic power spectrum appear[15],[16], resulting in the incorrect turbulent properties. In this study, Slot-Correlation method is used, in which no correction is needed to obtain the correlation coefficient based on randomly sampled signals[15]-[17]. In this approach, the correlation plane is slotted to
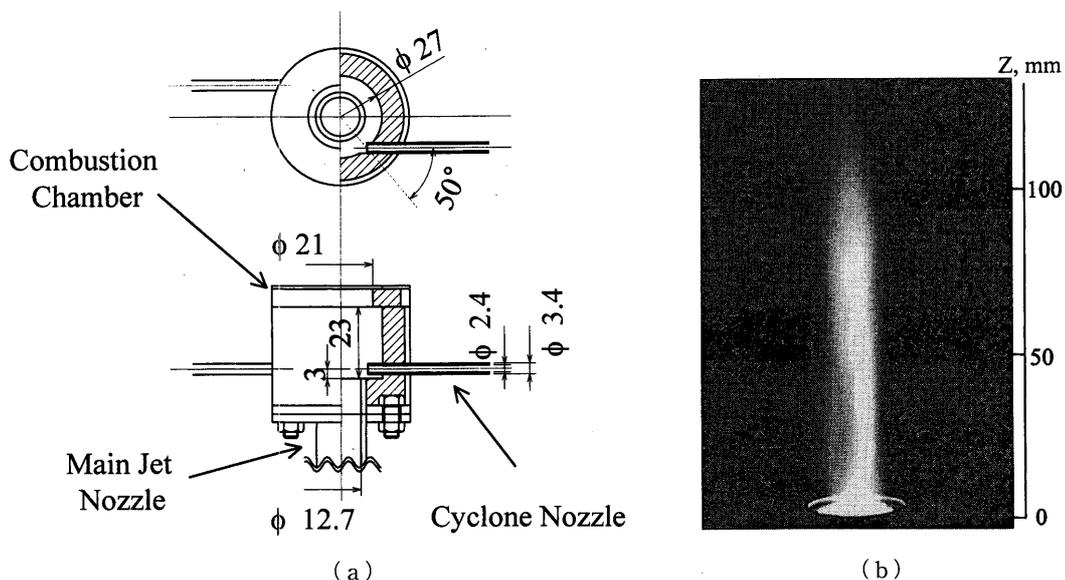

(a)

(b)

Fig. 1 (a) Cyclone-jet combustor, and (b) direct photograph of flame ($U_m=10$ m/s, $\phi_m=0.75$)

estimate the correlation by equispaced lag times of $\tau_k = k\Delta\tau$, where $\Delta\tau$ is the slot width. The correlation coefficient is obtained by

$$R_{u'u'(k\Delta\tau)} = \frac{\frac{1}{N_{k\Delta\tau}}\Sigma\{u'(t_i)u'(t_j)\}_{(k\Delta\tau)}}{\frac{1}{N}\Sigma\{u'(t_i)\}^2}$$

$$\tau_k - \Delta\tau/2 \leq (t_j - t_i) \leq \tau_k + \Delta\tau/2 \qquad (1)$$

where u' is the velocity fluctuation and t_i and t_j is the time of velocity observed. This means that all cross products of $u'(t_i)u'(t_j)$ contribute to $R(\tau_k)$ when the delay period satisfies $\tau_k - \Delta\tau/2 < (t_j - t_i) < \tau_k + \Delta\tau/2$.

The Slot-Correlation method has been already proposed, but there are little researches to validate this method. Even in the some papers related with experimental techniques, there is no comparison between results of the Slot-Correlation method and conventional sampling, except for short communication of Ref.(22). Here, we analyze velocity data in highly turbulent flow. LDV system is composed of a 0.3 mW Argon ion laser and a Doppler signal analyzer (TSI IFA755) to measure the axial component of the velocity. Seeded particles are talc powder (Takehara Kagakukogyo, Inc. HE-5). A hot wire anemometer is also used for evaluating the system.

2.3 Approach for determination of reaction zone thickness

We use an electrostatic probe to characterize the local reaction zone, which specifies the reaction region where the ion-electron formation and recombination reactions occur. The ion probe consists of a platinum wire sensor of 0.1 mm in diameter and 0.5 mm long. The sensor projected from a fine quartz tube over which a water-cooled tube is fitted to prevent the quartz tube from the thermal dielectric breakdown.

The potential drop across the load resistance is amplified to obtain ion currents, stored in the computer. The sample frequency is 50 kHz, which may not be enough to follow the variations of ion current signals. However, as explained later, we only need the probability of reaction zone existing to estimate the reaction zone thickness[14]. Then, data number is important to determine the properties statistically.

Here, the procedure of our proposed approach is shown. It should be noted that the ion current collected by an electrostatic probe depends on the flow velocity and flame curvature[13], and it is difficult to derive flame characteristics directly. However, at least, we can specify the reaction zone by examining the region of high ion concentration. We consider the reaction variable, a, whose value is unity inside the reaction zone, and zero outside the reaction zone. It should be noted that this reaction variable is different from the so-called progress variable, c, whose value is zero in unburned gas and unity in burned gas[23].

For example, let us consider a laminar flame (see Fig. 2(a)). We assume that the flame is stationary and the reaction zone is located between $x=0$ and $x=\delta$, where x is the coordinate normal to the flame front, and δ is the reaction zone thickness. In this case, if we integrate a along the x-axis, we can obtain the reaction zone thickness.

$$\int_{-\infty}^{+\infty} a(x)dx = \int_0^\delta a(x)dx = \int_0^\delta 1\,dx = \delta. \qquad (2)$$

However, since the turbulent flame is always fluctuating, it is impossible to determine one fixed coordinate normal to the flame front. Here, we take the coordinate normal to the mean flame front, x^*(see Fig. 2 (b)). If the flame is inclined to x^*-axis at one moment, we obtain $\delta^* = \delta/\sin\theta$ by this integration,
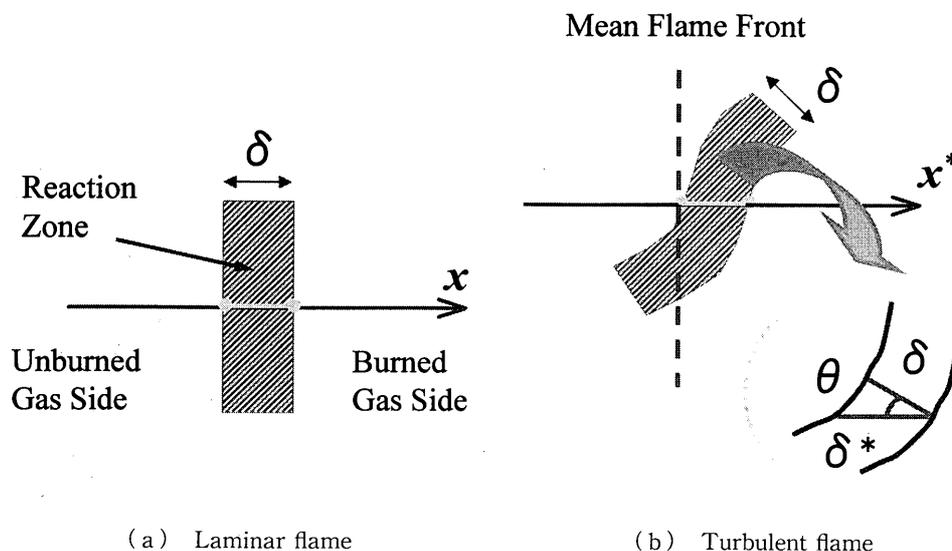
Mean Flame Front

(a) Laminar flame

(b) Turbulent flame

Fig. 2 Flame motion and reaction zone thickness

where θ is the acute angle between the mean flame surface and the normal to the instantaneous flame front at a crossing point. We introduce the probability of reaction zone existing, p. By time-averaged value of reaction variable, p is determined at specified location.

$$p(x^*)=\frac{1}{T}\int_0^T a(x^*,\,t)dt \qquad (3)$$

where T is the period of time averaging. Then, the mean value of δ^* is obtained by

$$\begin{aligned}\delta_m^*&=\frac{1}{T}\int_0^T \delta^*(t)dt\\&=\frac{1}{T}\int_0^T\int_{-\infty}^{+\infty} a(x^*,\,t)dx^*dt\\&=\int_{-\infty}^{+\infty}\frac{1}{T}\int_0^T a(x^*,\,t)dtdx^*\\&=\int_{-\infty}^{+\infty} pdx^*,\end{aligned}\qquad (4)$$

where the subscript, m, means the time averaged value. Assumed that the local flame structure is only wrinkled by turbulence, the reaction zone thickness remains undisturbed. The thickness can be obtained through the correction of the flame inclination by,

$$\begin{aligned}\delta_m&=\delta_m^*\times\overline{\sin\theta}\\&=\int_{-\infty}^{+\infty} pdx^*\times\overline{\sin\theta}.\end{aligned}\qquad (5)$$

Therefore, if we determine the probability of reaction zone existing and the inclination angle, we can estimate the reaction zone thickness. Since this approach is based on a point-measurement, it is easy to collect enough data for statistical reliability.

3. Results and Discussion

3.1 Flow field and phase diagram

First, we obtain the turbulent properties. Figure 3 shows the velocity fluctuation obtained at $r=0$ mm, $Z=60$ mm, $U_m=30$ m/s in cold flow. The velocity signals are shown by real data. To make clear errors in conventional sampling, the velocity is estimated at sampling rate of 15 kHz by two ways, holding the signal or linear interpolation. So far, these conventional samplings have been adopted without any evaluation in LDV measurements. When the signal is hold, unrealistic fluctuation of constant velocity appears at $t=0$ - 0.5 or 1.7 - 2.3 ms (Fig. 3(a)). On the other hand, the velocity fluctuation is reduced with linear interpolation, especially at $t=0.8$ - 1.3 ms (Fig. 3(b)). To evaluate these errors quantitatively, we obtain the integral time scale, L_t. Integral length scale, L_x is estimated by Taylor hypothesis, and Kolmogorov scale, η, is evaluated by $\eta=L_x\cdot(L_x\cdot u'/\nu)^{-0.75}$ in this study. Results are shown in Table 1. Those obtained by the hot wire anemometer are also shown, which is considered to be the correct value in this experiment. Also, we estimate turbulent

Table 1 Turbulent properties

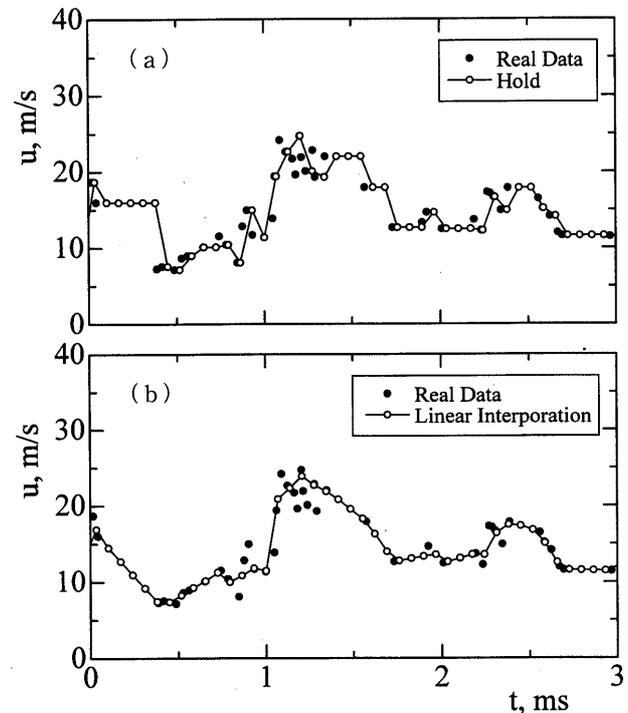|	U, m/s	u', m/s	L_t, ms	L_x, mm	η, μm
Linear	15.26	4.82	0.65	9.9	25
Hold	15.30	5.14	0.59	9.0	23
Slot	16.79	5.02	0.45	7.6	22
Hot wire	17.67	4.95	0.45	7.9	23

Fig. 3 Measured velocity fluctuation and data points by (a) hold, (b) linear interpolation in cold flow ; r $=0$ mm, $Z=60$ mm, $U_m=30$ m/s

properties using the Slot Correlation method.

Results show that the RMS fluctuating velocity, u', is larger by holding the data, while smaller by linear interpolation. Due to these errors, estimated integral time scale and integral length scale are much larger. On the other hand, these values by the Slot Correlation method are close to those by the hot wire anemometer. It is reasonable, because there is no correction needed in the Slot Correlation method. Then, the Slot Correlation method is appropriate especially under highly turbulent condition where the larger velocity fluctuation is expected.

Next, we examine the flow field in combustion. To explain the flame structure in the cyclone-jet combustor, the axial profiles of time-averaged velocity, temperature, and ion current are examined. Figure 4 shows these profiles along the center axis for $U_m=10$ m/s. The velocity profiles in cold flow and combustion field are compared. As seen in this figure, the flow is largely changed with combustion. Compared with the mean velocity in cold flow, the velocity in combustion is almost constant even relatively down-
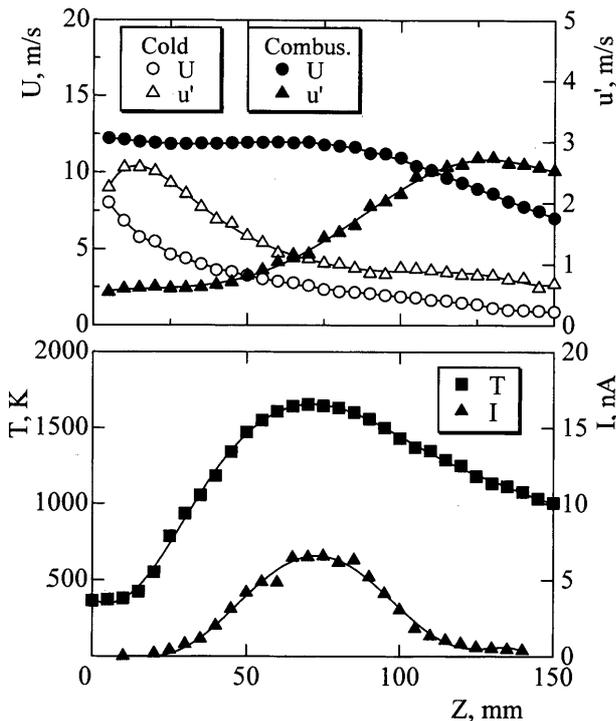
Fig. 4 Axial distributions of time-averaged velocity, temperature, and ion current; $U_m=10$ m/s, $\phi_m=0.75$

Fig. 5 Experimental conitions on phase diagram

stream, and it starts to decrease at $Z=70$ mm, with larger RMS fluctuating velocity. Around $Z=10$ - 30 mm, the temperature starts to increase monotonically, which corresponds to the preheat region. Since the ion current is high only in the reaction region, the reaction zone is mainly fluctuating around $Z=50$ - 100 mm.

To discuss the effect of turbulence on the reaction region, turbulent properties should be determined at the edge of the reaction region. Then, we obtain these values before ion current starts to increase. Figure 5 shows the experimental conditions on phase diagram. The laminar burning velocity, S_L, is referred to experimental data[24], and δ_L is the Zeldovich thickness. The axial positions where we obtain the turbulent properties are shown in this figure. The turbulent Reynolds number is 150 to 350 in this experiment. It is found that the condition of $U_m<15$ m/s belongs to the flamelet regime, and that of $U_m>20$ m/s belongs to the distributed reaction zone regime.

3.2 Turbulence and reaction zone thickness

To estimate the reaction zone thickness, we need to obtain the mean value of the inclination angle, θ. This angle appears as the flamelet crossing angle in Bray-Moss-Libby (BML) model[23], which is defined as the acute angle between the mean progress variable contour and the normal to the instantaneous front surface. In the work of Chew et al.[25], the overall mean cosine value of θ is found to be 0.5 for Bunsen
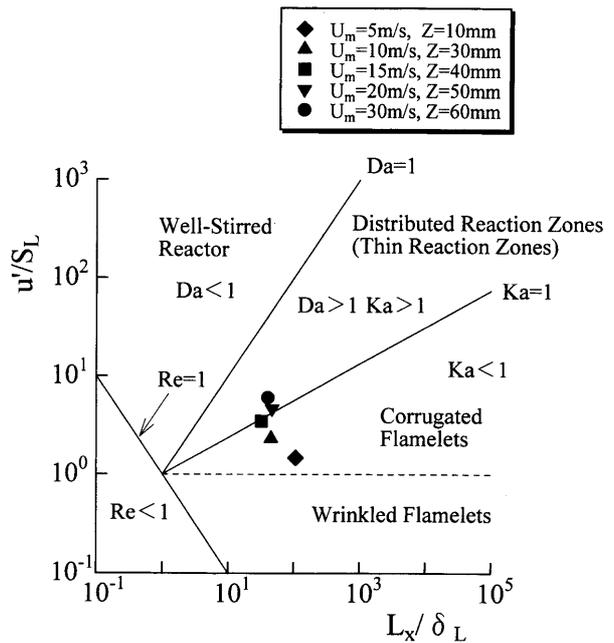
flame. Recently, Shy et al. have obtained this value for turbulent premixed flames near iso-tropic turbulence[26]. The reported value is 0.58 - 0.65. Hence, we obtain the mean value of cos θ based on 200 tomographic images. Results are shown in Fig. 6, along with the typical tomographic image. It is found that when the velocity is low, the mean value of crossing angle depends on the axial position, but it is almost constant for $U_m>10$ m/s. This constant value is close to that of Bunsen flame[25]. Unfortunately, for $U_m>20$ m/s, the crossing angle can not be determined, because the flame front is not clear due to the smaller scale of turbulence. Then, for $U_m=20$ and 30 m/s, we correct the flame inclination by using θ for $U_m=15$ m/s, assuming the constant flamelet crossing angle.

Next, we determine the probability of reaction zone existing, $p(x^*)$. We need to know whether the reaction occurs or not at the specified time and space. We use simple threshold procedure. The ion current signals are binarized with reaction variable, a, whose value is unity or zero. This procedure is shown in Fig. 7 for $U_m=15$ m/s at $r=9$ mm, $Z=20$ mm. If the ion current is higher than the threshold, it is considered that the probe is located in the reaction region and the reaction variable is unity, whereas if the ion current is lower than the threshold, a is zero. According to Okamoto et al.[13], ion current signal depends on the angle between the flame and the ion probe, and takes its maximum when the flame front is parallel to the sensor. Then, we adopt the half value of maximum ion current as threshold, I_{th}, because the width at half height is considered to be the time when the reaction zone passes the sensor. As seen in Fig. 7, some peaks
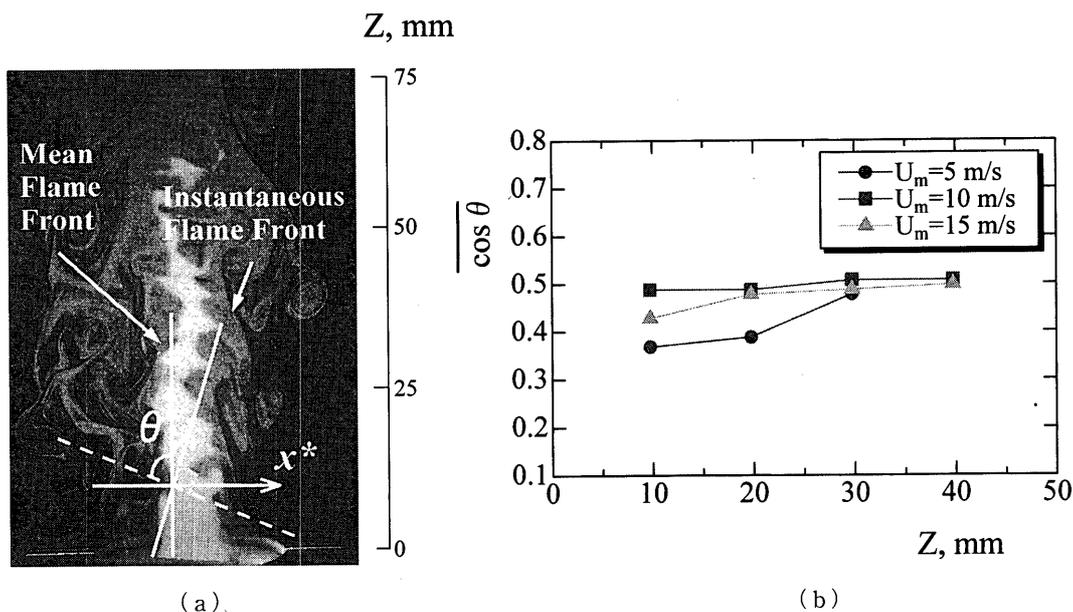
Z, mm

(a)

(b)

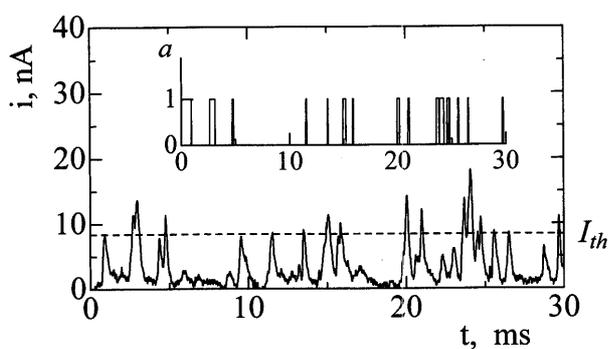Fig. 6　(a) Tomographic image and (b) mean crossing angle of θ ; $(U_m=10$ m/s, $\phi_m=0.75)$

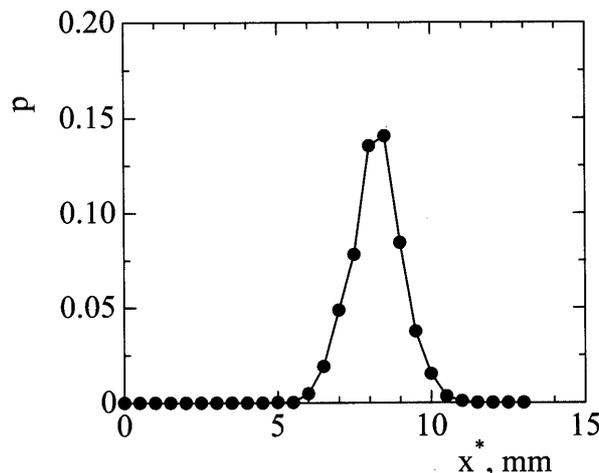Fig. 7　Signal waveform of ion current and reaction variable $(U_m=15$ m/s, $r=9$ mm, $Z=20$ mm, $\phi_m=0.75)$

Fig. 8　Distribution of probability of reaction zone existing, $p(U_m=15$ m/s, $Z=20$ mm, $\phi_m=0.75)$

of signals are lower than threshold, which means that the flame does not pass the sensor completely or the flame passes inclined to the sensor. It should be noted that the sensor length of is 0.5 mm, much larger than its diameter of 0.1 mm. These lower peaks are not counted, because the spatial resolution does not correspond to the diameter of the probe : otherwise the flame is thicker due to the lower spatial resolution. The obtained reaction variable, a, is also shown in this figure.

Finally, we determine the probability of reaction zone existing, p, by time-averaging procedure. Typical distribution of p is shown in Fig. 8, which is obtained for $U_m=15$ m/s at $Z=20$ mm. The x^*-coordinate is chosen by tomographic images, and $x^*=0$ is the center axis of the combustor. The probability of reaction zone existing is determined by 65 000 data sampling. It is found that the reaction zone is fluctuating at $x^*=6$ - 10 mm. By integration of p along x^*-axis, the reaction zone is estimated.

Figure 9 shows the obtained reaction zone thickness for $U_m=5$ m/s at $Z=10$ mm as functions of equivalence ratio. The thickness of a Bunsen flame $(U=1.8$ m/s, $\phi=0.85$, $Re=2\,000)$ is shown, which is also obtained in this study. The error (scattering) is about 10 to 20%, and only mean value is shown in Fig. 9. To validate our approach, we compare the results with Zeldovich thickness or experimentally obtained flame thickness by Yamaoka and Tsuji[24]. Here, we obtain non-dimensionalized thickness normalized by that of $\phi=1$, because the normalized thickness is not largely changed even if different threshold is adopted. Results show that the thickness of Bunsen flame is almost the same as that in a cyclone-jet combustor. Also, the dependence on equivalence ratio is quite similar for all cases. Therefore, it is considered that the reaction zone thickness with turbulence can be
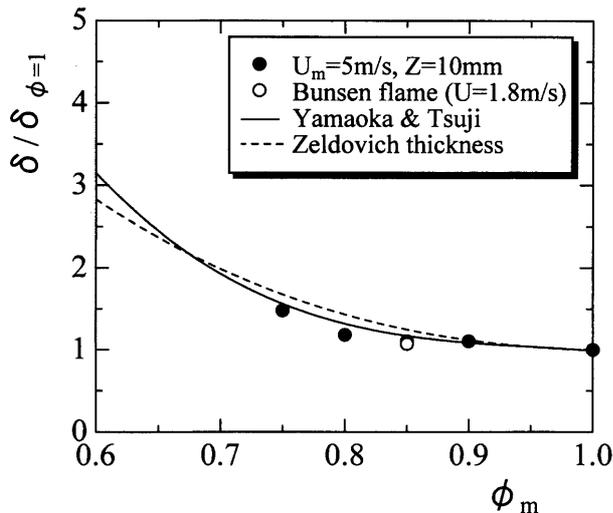
414

Fig. 9 Variations of reaction zone thickness with equivalence ratio

Fig. 10 Variations of reaction zone thickness with exit velocity; $\phi_m = 0.75$

discussed by our proposed approach.

Next, we change the exit velocity with constant equivalence ratio. Results are shown in Fig. 10, obtained at $Z = 20$ mm, $\phi_m = 0.75$. The Karlovitz number, $Ka(=(\delta_L/\eta)^2)$, is also shown. In this experiment, the values of η are 159, 92, 63, 55, 44 μm for $U_m = 5, 10, 15, 20, 30$ m/s, respectively. It is found that the reaction zone thickness is almost constant, even when the exit velocity is increased. This result is contrary to the hypothesis that predicts "thickened flames" for $Ka > 1$ (Klimov-Williams criterion).

Recently, it has been reported that the reaction zone remains thin with thicker preheat zone for $Ka > 1$[6]–[8]. Based on experimental data by Chen et al., the measured preheat zone thickness of turbulent flames is almost five times larger than that of a laminar flame[27]. It should be noted that, since the reaction zone thickness is much smaller than preheat zone thickness, this finding is obviously reasonable if the turbulence scale is smaller than preheat zone thickness, but larger than reaction zone thickness. As a result, the turbulence can not affect the reaction zone structure. However, we could confirm that the reaction zone thickness does not change even though Kolmogorov scale is smaller than the reaction zone thickness.

It may be noticed that, since our approach is based on the assumption that the flame is only inclined by turbulence, it can not be applied to the distributed reaction zone regime, where many small-scaled distributed reaction regions may exist. In this case, there may be lack of spatial resolution, and the estimated thickness by our method is not correct quantitatively. But, at least, the reaction zone thickness should be thicker if the reaction region were distributed. As for the spatial resolution, the experimentally obtained
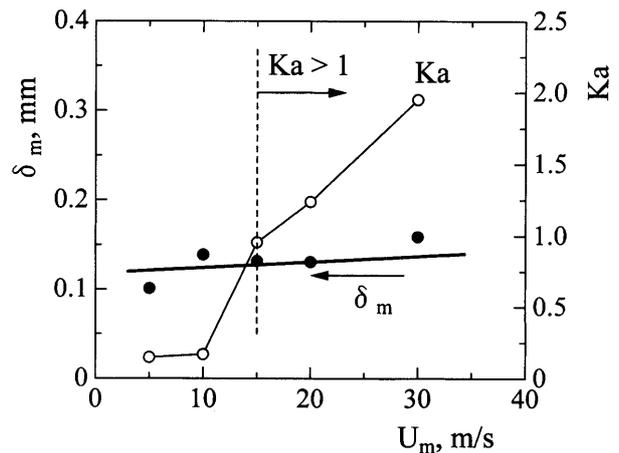
thickness in Fig. 10 is almost the same order of the diameter of the probe, 0.1 mm. However, since the turbulent flame is always inclined to the coordinate normal to the mean flame front, the instantaneous thickness across x^*-axis is much larger than the probe diameter. Also, based on tomographic images, the multiple flame crossing of corrugated flame is rare event at $Z < 30$ mm. Therefore, it could be concluded that the laminar flamelet structure remains even under highly turbulent conditions.

4. Conclusions

We have investigated the premixed flame structure in highly turbulent flow with a cyclone-jet combustor. With Mie scattering imaging, we have obtained tomographic images of flames. Based on the turbulent properties determined by Slot-Correlation method, the condition of $U_m < 15$ m/s belongs to the flamelet regime, and that of $U_m > 20$ m/s belongs to the distributed reaction zone regime on the combustion diagram. We have determined the reaction zone thickness using our new proposed approach, based on the probability of reaction zone existing.

Results show that the dependence of reaction zone thickness on equivalence ratio is very similar to those of the experimental values by Yamaoka and Tsuji or the Zeldovich thickness. When the exit velocity is increased, the reaction zone thickness is almost constant for $Ka > 1$. Hence, the persistence of laminar flamelet structure is observed, even when the Kolmogorov scale is smaller than reaction zone thickness. It could be concluded that the reaction region remains undisturbed with thin reaction zone under highly turbulent conditions. These results are useful for modeling the turbulent combustion.

References

(1) Borghi, R., Recent Advances in Aeronautics Science, (1985), pp. 117-134.

(2) Peters, N., Proc. Comb. Inst., Vol. 21 (1986), pp. 1231-1250.

(3) Yoshida, A., Proc. Comb. Inst., Vol. 22 (1988), pp. 1471-1478.

(4) Yoshida, A., Narisawa, M. and Tsuji, H., Proc. Comb. Inst., Vol. 24 (1992), pp. 519-525.

(5) Ikeda, Y., Kojima, J., Nakajima, T., Akamatsu, F. and Katsuki, M., Proc. Comb. Inst., Vol. 28 (2000), pp. 343-350.

(6) Mansour, M.S., Peters, N. and Chen, Y.C., Proc. Comb. Inst., Vol. 27 (1998), pp. 767-773.

(7) Peters, N., J. Fluid Mech., Vol. 384 (1999), pp. 107-132.

(8) Plessing, T., Kortschik, C., Peters, N., Monsour, M.S. and Cheng, R.K., Proc. Comb. Inst., Vol. 28 (2000), pp. 359-366.

(9) Sankaran, V. and Menon, S., Proc. Comb. Inst., Vol. 28 (2000), pp. 203-209.

(10) Tanahashi, M., Fujimura, M. and Miyauchi, T., Proc. Comb. Inst., Vol. 28 (2000), pp. 529-535.

(11) Buschmann, A., Dinkelacker, F., Schafer, T. and Wolfrum, J., Proc. Comb. Inst., Vol. 26 (1996), pp. 437-445.

(12) Cheng, Y.C. and Bilger, R.W., Proc. Comb. Inst., Vol. 28 (2000), pp. 521-528.

(13) Okamoto, K., Furukawa, J. and Hirano, T., Nensyo no Kagaku to Gijutsu, (in Japanese), Vol. 6 (1998), pp. 45-53.

(14) Yamamoto, K., Nishizawa, Y. and Onuma, Y., Journal of The Korean Society of Combustion, Vol. 6, No. 2 (2001), pp. 36-42.

(15) Gaster, M. and Roberts, J.B., J. Inst. Maths. Applics., Vol. 15 (1975), pp. 195-216.

(16) Adrian, R.J. and Yao, C.S., Experiments in Fluids, Vol. 5 (1987), pp. 17-28.

(17) Roberts, J.B. and Ajmani, D.B.S., IEE Proceedings, Vol. 133, Pt. F, No. 2 (1986), pp. 153-162.

(18) Saito, T., Ikeda, Y., Hosokawa, S., Nakajima, T., Kurosawa, Y. and Tamaru, T., Trans. Jpn. Soc. Mech. Eng., (in Japanese), Vol. 65, No. 633, B (1999), pp. 1813-1821.

(19) Yamamoto, K., Achiha, T. and Onuma, Y., Trans. Jpn. Soc. Mech. Eng., (in Japanese), Vol. 65, No. 637, B (1999), pp. 3185-3190.

(20) Yamamoto, K. and Nishizawa, Y., Trans. Jpn. Soc. Mech. Eng., (in Japanese), Vol. 68, No. 665, B (2002), pp. 238-245.

(21) Yamamoto, K., Nishizawa, Y. and Onuma, Y., Trans. Jpn. Soc. Mech. Eng., (in Japanese), Vol. 68, No. 666, B (2002), pp. 603-609.

(22) vab Maanen, H.R.E., Nobach, H. and Benedict, L.H., Meas. Sci. Technol., Vol. 10 (1999), pp. 4-7.

(23) Bray, K.N.C., Moss, J.B. and Libby, P.A., Combust. Flame, Vol. 61 (1987), pp. 127-142.

(24) Yamaoka, I. and Tsuji, H., Proc. Comb. Inst., Vol. 20 (1984), pp. 1883-1892.

(25) Chew, T.C., Bray, K.N.C. and Britter, R., Combust. Flame, Vol. 80 (1990), pp. 65-82.

(26) Shy, S.S., Lee, E.I., Chang, N.W. and Yang, S.I., Proc. Comb. Inst., Vol. 28 (2000), pp. 283-289.

(27) Chen, Y.C. and Mansour, M.S., Proc. Comb. Inst., Vol. 27 (1998), pp. 811-818.